DIRAC Note 2013-02

CERN-November 19, 2013

T8 Beam Parameters and $\pi^+\pi^-$ pairs production on Pt foil

L. Afanasyiev, V. Brekhovskikh, D.Drijard, O.Gortchakov, L. Nemenov,
M. Pentia, T.Vrba, V. Yazkov

Abstract

The PS proton beam position and beam size in the T8 channel, incident on the DIRAC target and Pt foil, have been evaluated. The obtained parameters were used to evaluate the ratio between $\pi^+\pi^-$ pairs produced by the beam halo and the $\pi^+\pi^-$ pairs produced by $A_{2\pi}$ break-up in the Pt foil.

1. Introduction

During 2011 and 2012 DIRAC runs experiments were performed to observe long-lived $A_{2\pi}$ by detecting atomic pairs produced by the long-lived $A_{2\pi}$ break-up in a Pt foil. One of the main sources of the background pairs with similar properties are Coulomb $\pi^+\pi^-$ pairs produced in the Pt foil by protons from the primary beam halo. For this background evaluation it needs to know the intensity of the proton flux crossing the Pt foil. The flux depends both on the distance Δy between proton beam axis and Pt foil edge and on the beam intensity distribution in the vertical plane.

In the DIRAC experiment all the measurements were done on the T8 channel proton beam.

- In 2011 the vertical proton beam intensity distribution has been probed with Cu wire.
- In 2011 and 2012 the proton beam position on the target was monitored in off-line analysis and, if necessary, it was corrected.

- Also in 2012 it was studied the influence of the Δy vertical displacement of the proton beam on the cumulative proton beam interaction probability to evaluate the proton beam intensity distribution in the vertical plane.
- Based on these measurements, the ratio of $\pi^+\pi^-$ Coulomb pairs produced by proton beam halo in Pt foil and $\pi^+\pi^-$ atomic pairs from long-lived $A_{2\pi}$ break-up on Pt foil was evaluated.

2. Proton beam position during 2012 Run.

The proton beam position of the PS T8 channel during 2012 Run was evaluated for each run by reconstructed tracks in off-line analysis with DC and SFD coordinates data. The result is shown in **Figure 1**. We can see that maximum proton beam axis deviation on *y* direction is 0.4*mm*.
The *mean value* and *standard deviation* for *x* and *y* coordinate beam position is:

$$\mu_x \pm \sigma_x = -1.04 \pm 0.68\ mm$$

$$\mu_y \pm \sigma_{yx} = 1.99 \pm 0.26\ mm$$

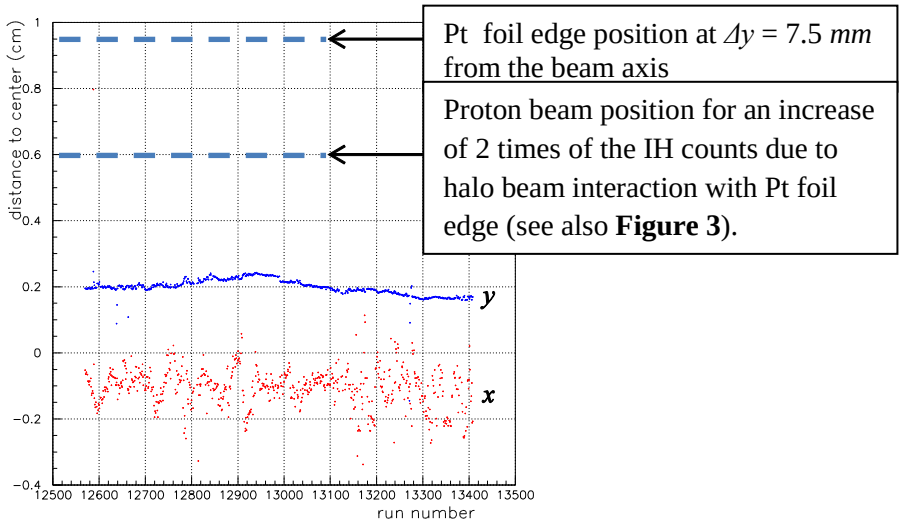

Figure 1. *y* - and *x* - position of the proton beam in 2012 Run

3. Cumulative measurement of the proton beam intensity *y* distribution

The proton beam intensity vertical distribution was studied in the 2012 run [1]. For this aim, the beam was moved on *y*-direction and its position measured on a scintillator screen placed in the target position (the distance between Be target and Pt foil is 100*mm*). With established Δy position of the beam, the screen was removed and the proton beam interaction with Pt foil was measured. The beam particles interaction with the Pt foil (placed at *y*=7.5*mm* from the beam axis) produces secondary particles flux which was measured in *y*-strips IHA7 and IHA8 of the Ionization Hodoscope (see **Figure 2**).

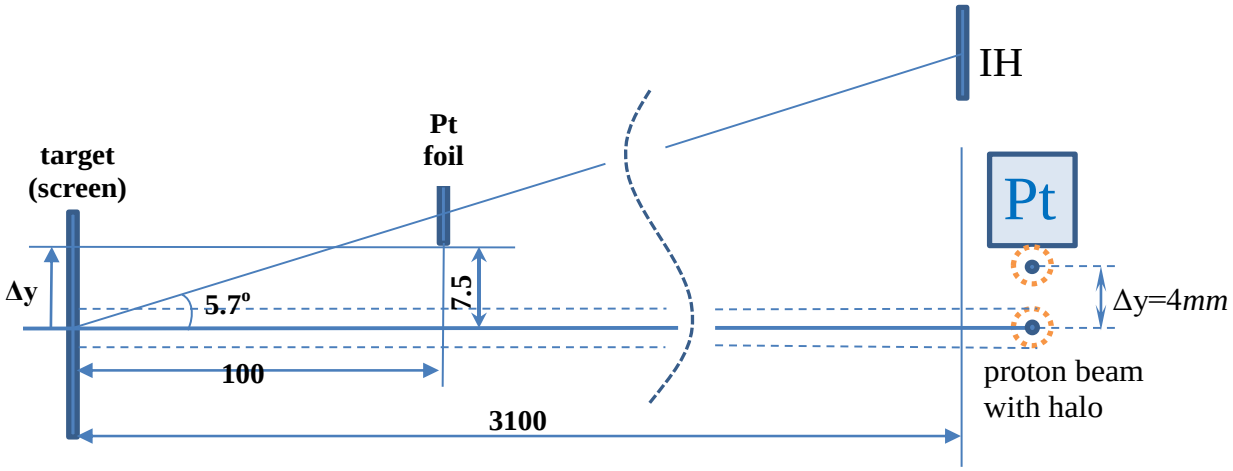

Figure 2. Measurement of the proton beam halo interaction with Pt foil (located at Δy = 7.5*mm* from the beam axis). The counting rate of the secondaries produced in Pt foil is measured by IHA7 and IHA8 strips of the Ionization Hodoscope.

As the proton beam is moved upward, the halo components begin to interact with the lower edge of the Pt foil. The secondary particle production rate is proportional to the fraction of the proton beam interaction with Pt foil. As the proton beam position is higher, more incident protons are interacting with the Pt foil and the corresponding IH counting rate increases (see **Figure 3**) until it reaches saturation level when full proton beam crosses the foil.

It is clear that at Δy=2*mm* the proton beam halo does not interact with the Pt foil and at Δy=4*mm* the count is still at the background level. This way, the measured counting rate integrates the proton beam as the *y* beam position is moved up.

Y (mm)	IHA7 (counts)	IHA8 (counts)
0	6220	5668
2	6337	5428
2	6474	5569
4	11802	9899
4	9249	8262
6	58286	47985
6	61676	58194
8	239810	199857
8	235995	199198
10	583531	484360
10	572517	476049
12	670405	558476

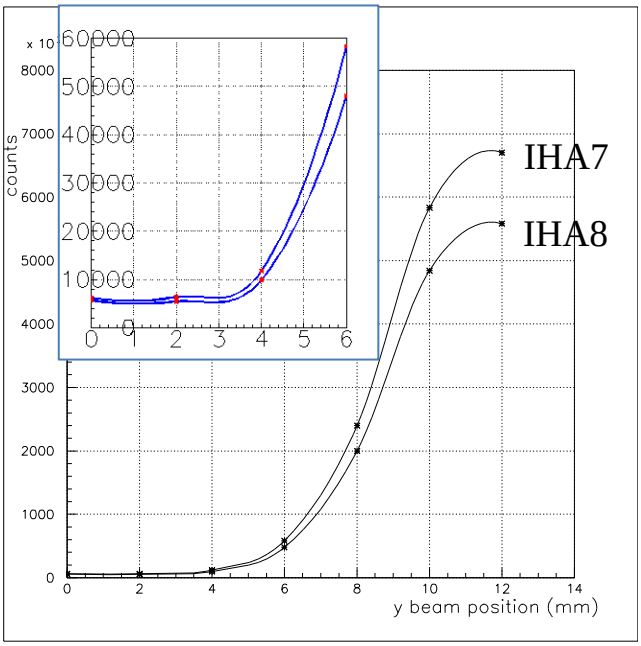

Figure 3. Contribution of the proton beam halo measured by IHA7 and IHA8 strips, in the counting rate as a function of *y*-position of the beam.

3.1. Description of the cumulative bivariate Gauss distribution.

The transversal proton beam 2-dimensional distribution can be described by a *bivariate Gauss distribution* (see **Figure 4, 5**) with corresponding standard deviations σ_x and σ_y along x and y axes:

$$h(x,y)\cdot dS = f(x)\,g(y)\cdot dx\,dy = \frac{1}{\sigma_x\sqrt{2\pi}}e^{-\frac{(x-\mu_x)^2}{2\sigma_x^2}}\cdot dx\;\;\frac{1}{\sigma_y\sqrt{2\pi}}e^{-\frac{(y-\mu_y)^2}{2\sigma_y^2}}\cdot dy \qquad (1)$$

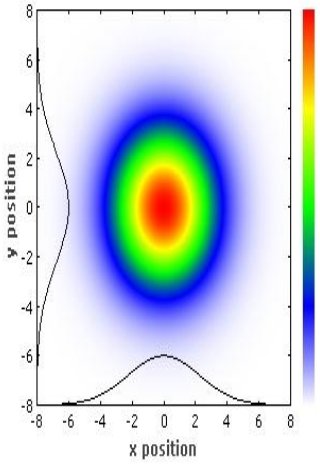

Figure 4. The qualitative picture of transversal distribution of the proton beam.

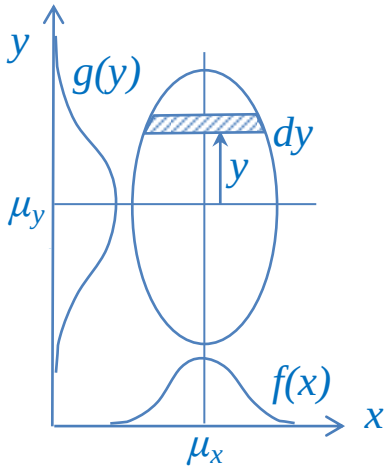

Figure 5. two-dimensional Gauss distribution with different σ_x and σ_y standard deviations.

As the cumulative measurement has been done along the y-positions, we must evaluate the integral for all x values from -∞ to +∞, and then for y from -∞ to $\mu_y+z\sigma_y$ with z standard deviations, for $h(x,y)$ bivariate Gaussian distribution (1),

$$\iint h(x,y)\cdot dx\,dy = \int_{\mu_x-s\sigma_x}^{\mu_x+s\sigma_x} f(x)\cdot dx \int_{\mu_y-z\sigma_y}^{\mu_y+z\sigma_y} g(y)\cdot dy \qquad (2)$$

The x-integral $\int_{\mu_x-s\sigma_x}^{\mu_x+s\sigma_x} f(x)\cdot dx$ is,

$$\int_{\mu_x-s\sigma_x}^{\mu_x+s\sigma_x} f(x)\cdot dx = \int_{\mu_x-s\sigma_x}^{\mu_x+s\sigma_x} \frac{1}{\sigma_x\sqrt{2\pi}}e^{-\frac{(x-\mu_x)^2}{2\sigma_x^2}}dx = \frac{1}{\sqrt{2\pi}}\int_{t=-s}^{t=+s} e^{-t^2/2}\,dt \xrightarrow[s\to\infty]{} \frac{1}{\sqrt{2\pi}}\sqrt{2\pi} = 1$$

We used the change of variable: $t=\frac{x-\mu_x}{\sigma_x}$; $dt=\frac{dx}{\sigma_x}$ and definite integral $\int_{-\infty}^{+\infty} e^{-t^2/2}\,dt = \sqrt{2\pi}$

The y-integral $\int_{\mu_y-z\sigma_y}^{\mu_y+z\sigma_y} g(y)\cdot dy$ is,

$$A(z) = \int_{\mu_y-z\sigma_y}^{\mu_y+z\sigma_y} \frac{1}{\sigma_y\sqrt{2\pi}}e^{-\frac{(y-\mu_y)^2}{2\sigma_y^2}}dy = \frac{1}{\sqrt{2\pi}}\int_{t_{min}=-z}^{t_{max}=+z} e^{-t^2/2}\,dt \xrightarrow[t_{min}\to-\infty]{} = \frac{1}{2}\left[erf\left(\frac{z}{\sqrt{2}}\right)+1\right] \qquad (3)$$

We used the change of variable: $t=\frac{y-\mu_y}{\sigma_y}$; $dt=\frac{dy}{\sigma_y}$ and indefinite integral $\int e^{-t^2/2} = \sqrt{\frac{\pi}{2}}erf\left(\frac{t}{\sqrt{2}}\right)$

The $A(z)$ dependence on z number of σ_y for interval limits -4σ_y to +4σ_y is presented in **Figure 6.b.**

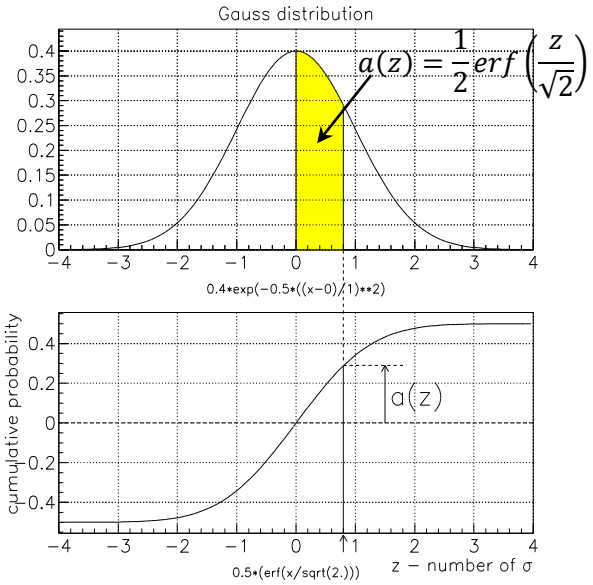

Figure 6.a. Error function component $a(z) = \frac{1}{2} erf\left(\frac{z}{\sqrt{2}}\right)$ of the *A(z)* cumulative probability (3).

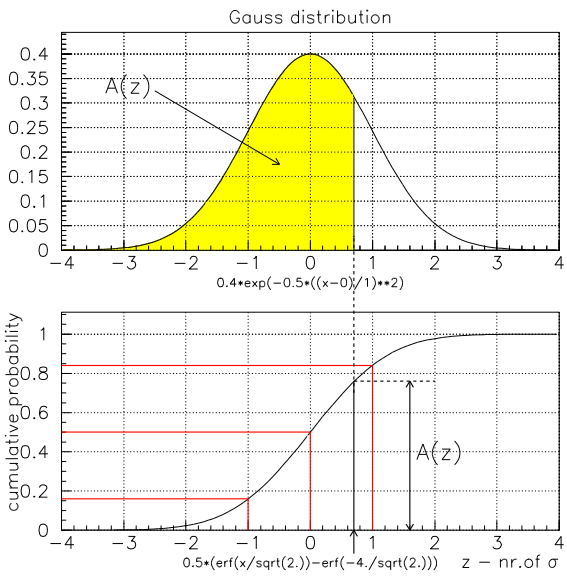

Figure 6.b. *A(z)* cumulative probability (3) dependence on $z\sigma_y$, for lower limit z_{min}=-4σ_y.
z-axis origin can be shifted by any value to fit to the measured beam position scale.

The experimental results **Figure 3** were compared with the theoretical *y*-dependence of the cumulative probability distribution **Figure 6.** The analysis of normalized and background corrected experimental data from **Figures 7, 8** shows the *y*-position (50% probability) at μ=8.6*mm.*

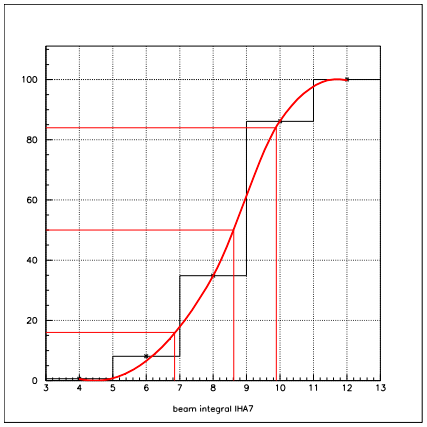

Figure 7. The IHA7 normalized experimental *counting rate* (background subtracted) dependence on *y*-position (*mm*) of the proton beam.

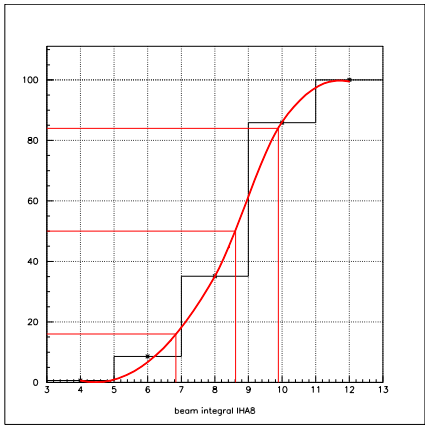

Figure 8. The IHA8 normalized experimental *counting rate* (background subtracted) dependence on *y*-position (*mm*) of the proton beam.

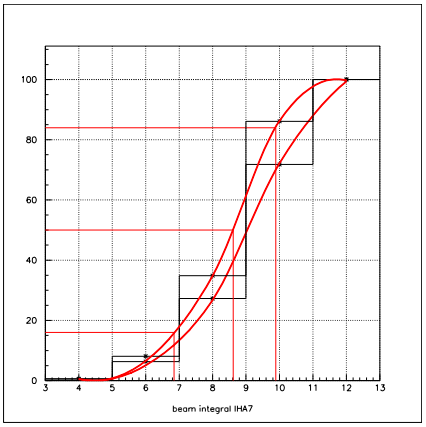

Figure 9. For higher *counting rate* with +10% and respective +20% for the last two points, due to dead time lost, the σ_y for 84% probability is higher.

From **Figure 6** we have for μ-σ_y a probability 16% and for μ+σ_y a probability 84%, which corresponds in **Figure 7** and **8** to an estimate $\sigma_y \approx$ 1.75*mm* and respective $\sigma_y \approx$ 1.25*mm*. The $\sigma_y \approx$1.25*mm* value is lowered due to electronics dead time. Even the dead time is not known, the qualitative correction **Figure 9** shows a higher σ_y. Nevertheless we take $\sigma_y \approx$1.75*mm* for upper value of the background estimation. It is the same as that obtained with target vertex position distribution [2].

4. Differential measurement of the proton beam transversal distribution

Direct probing of the incident proton beam size was done [3] by studying the interaction rate of a horizontal Cu wire, diameter 0.3*mm*, in the absence of target, as a function of its *y*-position. The measurements were done during the 2011 Run, with a Cu wire attached on the magnet yoke at about 40*mm* from target position and another one with a Cu wire attached on the Pt foil holder at about 100*mm* from the target.

The counting rate produced by the secondary particles generated in p – Cu and magnet yoke interaction was measured by IHA7 and IHA8 strips of the Ionization Hodoscope.

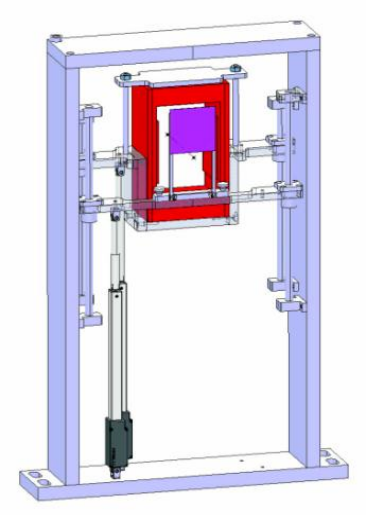

Figure 10. The magnet yoke (red) and Pt foil holder (purple) with individual devices for vertical movement of the two elements.

4.1. The measurement with Cu wire attached to the magnet yoke.

In the first set of measurements, the wire was fixed on the magnet yoke (face to target) located between target position and Pt foil (see **Figure 10** and **Figure 11**).

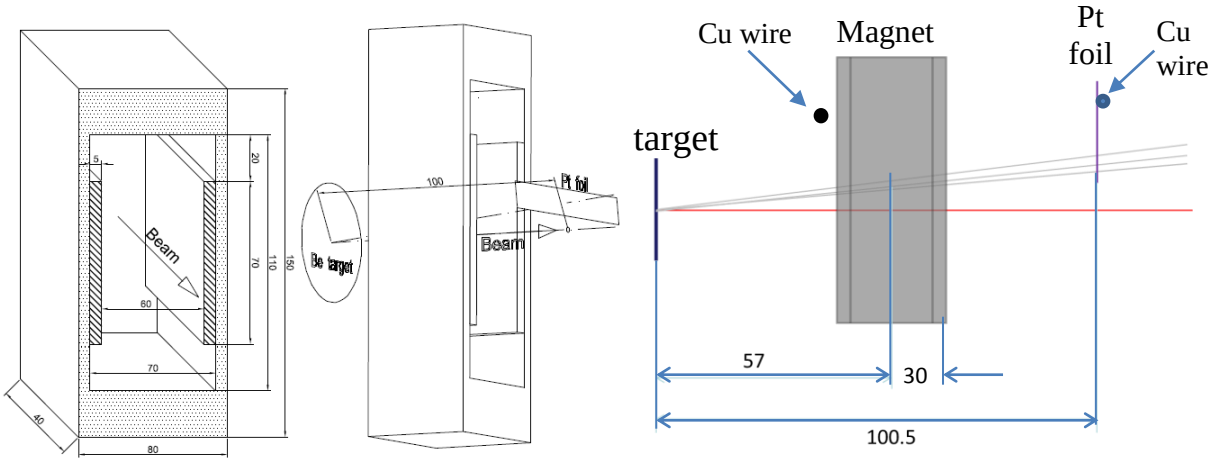

Figure 11. The magnet yoke with Cu wire and its position between target and Pt foil.

In the absence of target, the magnet yoke with Cu wire was moved downward (see **Figure 12**). The signal was collected by IHA7 and IHA8 strips of Ionization Hodoscope.

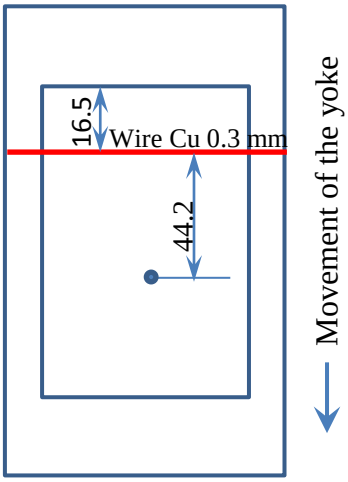

Figure 12. Cu wire position on magnet yoke at 44.20*mm* from proton beam.

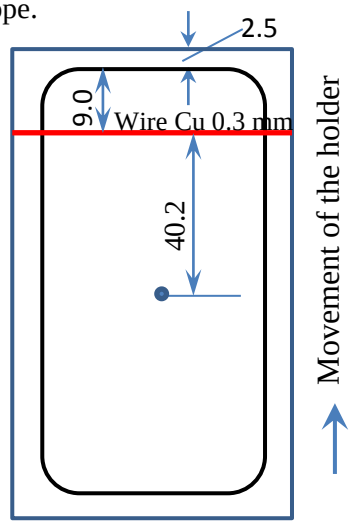

Figure 13. *Cu* wire position on the Pt foil holder at 40.2*mm* from proton beam.

Y-position	Counts
55	3977
56	4172
57	4096
58	4301
59	4206
60	4486
61	4695
62	4740
63	5162
64	6318
65	9372
66	21818
67	211479
68	56692
69	20994
70	17782
71	18963
72	22035
73	26391
74	31819
75	67483
76	134261
77	348840

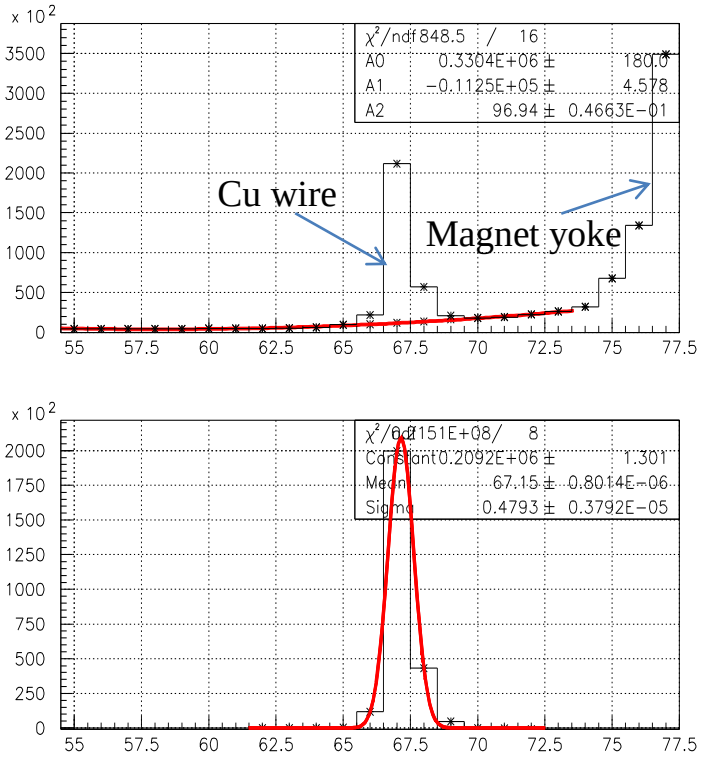

Figure 14. The counting rate (counts) dependence on *y*-position (*div* units) of the Cu wire (magnet yoke)

The result of these measurements is shown in **Figure 14**, as variation of the counting rate with *y* yoke position measured in *div* units (indication of the movement device). The peak at 67.15 *div* is

due to interaction of the proton beam with the Cu wire. Dependence of the mean counting rate on *y*-position of the Cu wire has been fitted by a Gaussian with a beam width σ=0.48 *div*. The counting rate increase at 75 *div* is due to proton beam interaction with magnet yoke.

4.2. The measurement with Cu wire attached to Pt foil holder

In the second set of measurements, the Cu wire was fixed on the Pt foil (see **Figure 13**).
In the absence of target, the Pt foil holder with *Cu* wire went up vertically. The signal was collected by IHA7 and IHA8 strips of the Ionization Hodoscope. The result of these measurements is shown in **Figure 15**, as dependence of the mean counting rate on the *y*-position of the Pt foil holder. Peak at 33.5 *div* is due to interaction of the proton beam with holder and that at 43.18 *div* is due to interaction with Cu wire.

The dependence of the mean counting rate on *y*-position around the 43.18 *div* peak was fitted with a Gaussian, see **Figure 15**. The beam width obtained is σ=0.72*div* for the Pt foil holder position.

Y-position (div)	Counts
25	4246
26	4560
27	4786
28	11166
29	21622
30	148881
31	264831
32	1352084
33	1537966
34	1546515
35	1002504
36	230980
37	97827
38	42162
39	29760
40	26598
41	30003
42	80158
43	193038
44	120328
45	31171
46	23697
47	22189
48	21771
49	22075

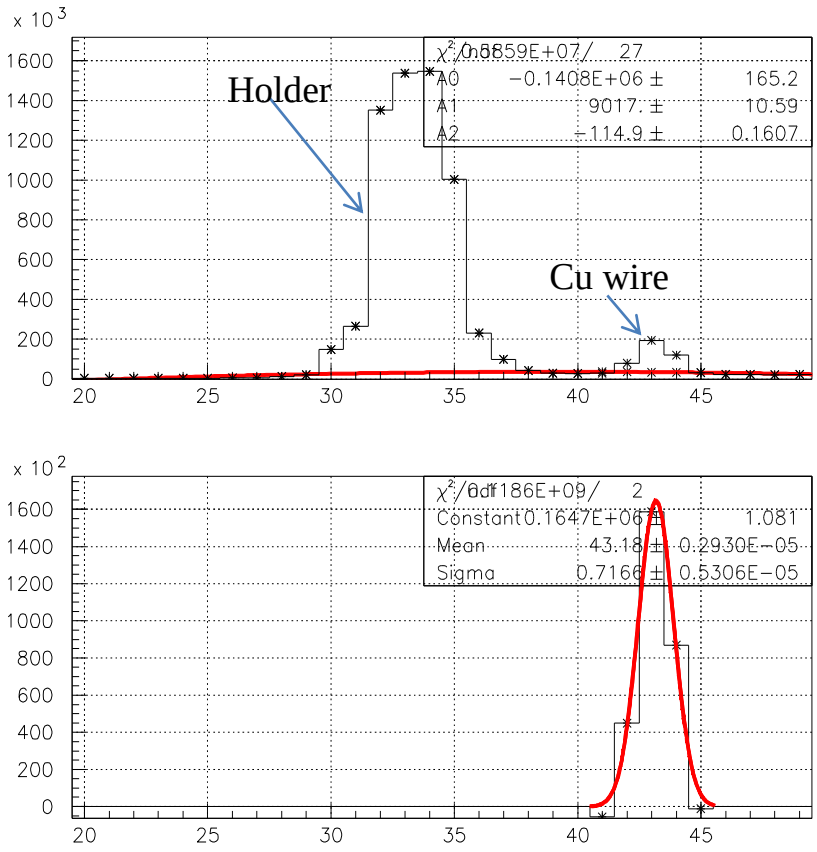

Figure 15. The counting rate dependence on the Pt foil holder *y*-position (div units). The peak at *y* = 33.40 *div* is due to proton beam interaction with holder and the one at *y* = 43.13 *div* due to interaction with Cu wire.

4.3. Calibration of the holder and magnet movement devices

The calibration measurement results are presented in **Table 1** [3].

Table 1

Elment position	Device units (div)
Magnet out off beam	135
Magnet working position	28
Magnet wire	67
Foil out off beam	5
Foil working position	88
Foil wire	43

- The magnet working position is at 28 *div* and the Cu wire position on magnet is at 67 *div*.
  The difference between these two positions is 44.20*mm*.
  So, the calibration constant for magnet movement device is 44.20/(67-28)=1.1 *mm*/*div*.
  The corresponding σ_y = 0.48 *div* x 1.1 *mm/div* = **0.53 *mm***.

- The Pt holder working position is at 88 *div*, and the corresponding Cu wire on holder position is 43 *div*. The difference between these two positions is 40.20*mm*.
  So the calibration constant for Pt holder movement device is 40.20/(88-43)=0.89 *mm/div*.
  The corresponding σ_y = 0.72 *div* x 0.89 *mm/div* = **0.64 *mm***.

- For Pt holder movement calibration one can also use the two peaks in the counting rate dependence on *y*-position of the holder (**Figure 14**). The holder signal is at 33.40 *div*. and the Cu wire signal is at 43.18 *div*. In the same time the distance between these two elements are (9.0+1.25)=10.25*mm* so we have 10.25/(43.18-33.40) = 1.05 mm/div.
  The corresponding σ_y = 0.72 *div* x 1.05 *mm/div* = **0.76 *mm***.

Conclusion.

The proton beam intensity *y*-distribution measurements show the σ_y (see **Table 2**).

Table 2

RUN	σ_y (*mm*)	Measurement type
2002	1.60	Tracking by offline analysis [2]
2012	0.76	Differential measurement with Cu wire [3]
2011	1.75	Cumulative measurement with Pt foil [1]

For background evaluation we will take the upper limit

$$\sigma_y = 1.75 \text{ mm} \tag{4}$$

which gives the overestimation value of the background due to proton beam halo.

5. Coulomb and atomic pairs production

The background particle production in Be target and Pt foil are evaluated.

5.1. Proton beam interaction with Be target

The number of produced $A_{2\pi}$ per one p-Be interaction is

$$N_A = K(q, q_L \le 1.5MeV/c, q_T \le 1.5MeV/c) \cdot N_C^{Be}(q_L \le 1.5MeV/c, q_T \le 1.5MeV/c)$$

or in brief

$$\mathrm{N}_A = K_{q_{cut}} \cdot N_{Cq_{cut}}^{Be} \qquad (5)$$

where

- q_L and q_T are the longitudinal and transversal component of relative momentum q in $\pi^+\pi^-$ pair CMS in the production point,
- $N_{Cq_{cut}}^{Be}$ – the produced Coulomb pairs number with $q_L \le 1.5MeV/c, q_T \le 1.5MeV/c$
- $K_{q_{cut}}$ – K factor for $q_L \le 1.5MeV/c, q_T \le 1.5MeV/c$

After production in the Be target some long-lived atoms will decay and some others will break-up (see lower part of **Figure 16**) in the Pt foil, producing n_A^{Pt} atomic pairs, the searched atomic pairs.

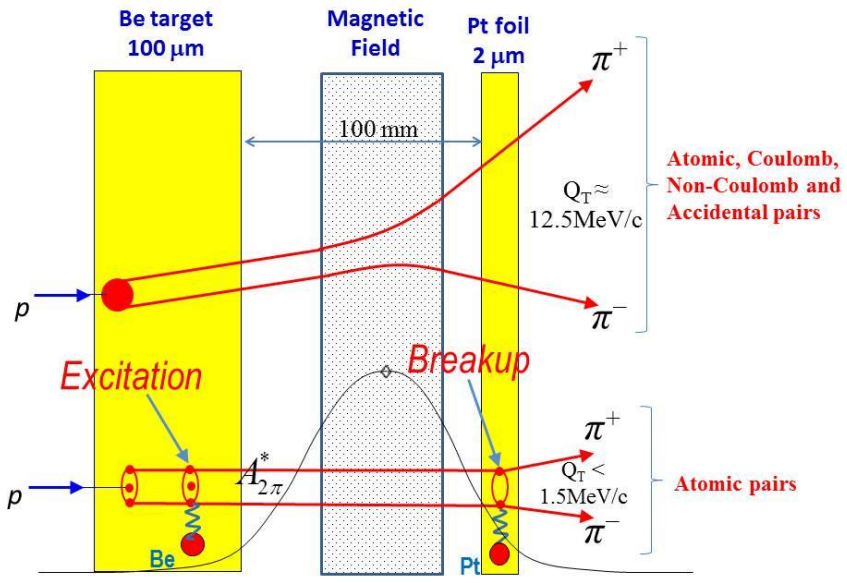

Figure 16. Production and observation of background events and long-lived $A_{2\pi}$ atoms with break-up Pt foil

By Monte-Carlo simulation, the total number of atomic pairs n_A^{Pt} produced in the Pt foil is,

$$n_A^{Pt} = 2.3 \cdot 10^{-2} \cdot N_A = 2.3 \cdot 10^{-2} \cdot K_{q_{cut}} \cdot N_{Cq_{cut}}^{Be} \qquad (6)$$

These searched events were detected and reconstructed.

The Monte-Carlo simulation shows that more than 95% of these pairs belong to the interval

$$Q_L \le 1.5MeV/c\,, \quad Q_T \le 1.5MeV/c \tag{7}$$

where Q_L and Q_T are the reconstructed relative momentum components in $\pi^+\pi^-$ CMS. Hence,

$$n_A^{Pt}(Q_L \le 1.5MeV/c, Q_T \le 1.5MeV/c) \approx 0.95\, n_A^{Pt} = 2.2\cdot 10^{-2}\varepsilon_A K(q, 1.5; 1.5)\, N_C^{Be}(q, 1.5; 1.5)$$

or in brief

$$n_{AQ_{cut}}^{Pt} = 2.2\cdot 10^{-2}\cdot \varepsilon_A \cdot K_{q_{cut}} \cdot N_{Cq_{cut}}^{Be} \tag{8}$$

where ε_A takes into account the pion decays, particle detection efficiency and requirement of the IH double ionization amplitude signal for events with one SFD column signal.

The number of produced $\pi^+\pi^-$ Coulomb pairs in Pt foil, with small q_L, q_T, is $N_{Cq_{cut}}^{Pt}$.

This pairs number is 1.8 times larger than $N_{Cq_{cut}}^{Be}$ with the same q_L, q_T [4].

$$N_{Cq_{cut}}^{Pt} = 1.8\ \cdot N_{Cq_{cut}}^{Be} \tag{9}$$

for $q_L, q_T \le 3MeV/c$.

After $\pi^+\pi^-$ pairs reconstruction, the number of Coulomb pairs $N_{CQ_{cut}}^{Pt}$ in the Q measured values interval $Q_L \le 1.5MeV/c, Q_T \le 1.5MeV/c$ is,

$$N_{CQ_{cut}}^{Pt} = \varepsilon_C \cdot \varepsilon_R \cdot N_{Cq_{cut}}^{Pt} \tag{10}$$

where

- ε_C takes into account the π^+ and π^- decays, detection efficiency and requirement of the IH double ionization amplitude signal for events with one SFD column signal.
- ε_R takes into account that some $\pi^+\pi^-$ paires with $q_L \le 1.5MeV/c, q_T \le 1.5MeV/c$, after reconstruction can go out of interval $Q_L \le 1.5MeV/c, Q_T \le 1.5MeV/c$ and some other $\pi^+\pi^-$ pairs from outside the interval, that is with $q_L > 1.5MeV/c, q_T > 1.5MeV/c$, can enter into interested interval $Q_L \le 1.5MeV/c, Q_T \le 1.5MeV/c$.

The ratio of the Coulomb pairs generated in Pt foil $N_{CQ_{cut}}^{Pt}$ according to (10) and the atomic pairs from long-lived breaking atoms $n_{AQ_{cut}}^{Pt}$ according to (8), is

$$\frac{N_{CQ_{cut}}^{Pt}}{n_{AQ_{cut}}^{Pt}} = \frac{\varepsilon_C \cdot \varepsilon_R \cdot N_{Cq_{cut}}^{Pt}}{2.2\cdot 10^{-2}\varepsilon_A \cdot\ K_{q_{cut}} \cdot N_{Cq_{cut}}^{Be}}$$

$$= \frac{\varepsilon_C \cdot \varepsilon_R \cdot 1.8}{2.2\cdot 10^{-2}\varepsilon_A \cdot\ K_{q_{cut}}} = 82 \cdot \frac{\varepsilon_C \cdot \varepsilon_R}{\varepsilon_A \cdot K_{q_{cut}}} \tag{11}$$

The strong proton interaction probability with Be target (thickness 100μm) is 10.6 times larger than that of Pt foil (thickness 2μm). With this in mind, the ratio (11) will be

$$\frac{N_{CQ_{cut}}^{Pt}}{n_{AQ_{cut}}^{Pt}} = 7.7 \cdot \frac{\varepsilon_C \cdot \varepsilon_R}{\varepsilon_A \cdot K_{q_{cut}}} \qquad (12)$$

If the proton flux across the Be target is I_{Be}, then the flux of the proton beam halo crossing the Pt foil I_{Pt} is a function of distance $\Delta y/\sigma_y$, where σ_y is the standard deviation of the Gauss distribution of the proton beam intensity in vertical plane.

The **Table 3** presents the ratio I_{Pt}/I_{Be} as a function of $\Delta y/\sigma_y$:

Table 3

$\Delta y/\sigma_y$	2.6	2.8	3.0	3.2	3.4	3.6	4.0
$I_{Pt}/I_{Be}\times10^{3}$	4.7	2.6	1.4	0.7	0.34	0.16	0.03
$N_{CQ_{cut}}^{Pt}/n_{AQ_{cut}}^{Pt}\times10^{-2}$	7.5	4.2	2.2	1.1	0.54	0.26	0.05

The working distance is Δy=7.5±0.5*mm*.

The σ_y of the proton beam intensity *y*-distribution is σ_y=1.75*mm*. So, for σ_y=1.75*mm* and Δy=7*mm* the $\Delta y/\sigma_y$=4.0

$$I_{Pt}/I_{Be} = 3 \cdot 10^{-5} \qquad (13)$$

The coefficients ε_R, ε_C, ε_A can be obtained by Monte Carlo simulation and $K_{q_{cut}}$ from Coulomb factor integration. Below is presented their crude estimations, and the upper limit of the ratio $N_{CQ_{cut}}^{Pt}/n_{AQ_{cut}}^{Pt}$ (12).

The ratio $\varepsilon_C/\varepsilon_A$ depends only on the probabilities of the Coulomb and atomic pairs crossing one column of SFD. In the case of atomic pairs this selection criterium decreases the $n_{AQ_{cut}}^{Pt}$ to 20%.

Supposing that the Coulomb pairs number does not decrease, the upper limit for $\varepsilon_C/\varepsilon_A$ is

$$\frac{\varepsilon_C}{\varepsilon_A} = 1.25 \qquad ??? \qquad (14)$$

The value of ε_R is about 1, and $K_{q_{cut}}$ is larger than 0.6. With these estimations, the ratio (12) is

$$\frac{N_{CQ_{cut}}^{Pt}}{n_{AQ_{cut}}^{Pt}} = 7.7 \cdot \frac{1.25}{0.6} = 16 \qquad (15)$$

Take into account the I_{Be}/I_{Pt} ratio for different values $\Delta y/\sigma$, the $N_{CQ_{cut}}^{Pt}/n_{AQ_{cut}}^{Pt}$ ratios are

presented in the **Table 3**.

For $\Delta y/\sigma_y$=4.0 the probability to generate $\pi^+\pi^-$ Coulomb pairs on Pt foil by protons from beam halo is two orders of magnitude smaller than long-lived atomic pairs produced by $\pi^+\pi^-$ atom break-up in the same foil.

5.2. Secondary particle interaction with Pt foil

The primary proton beam intensity is $I_p = 2.8 \cdot 10^{11} \frac{p}{spill}$, and the corresponding IH-XA-7 ionization hodoscope counting rate is $I_{IH} = 4.2 \cdot 10^5 \frac{part}{spill}$.

The ratio of Coulomb pairs generated in Pt foil $N_{CQ_{cut}}^{Pt}$ relative to atomic pairs number from long-lived breaking atoms $n_{AQ_{cut}}^{Pt}$ produced in Be target, according to (15) is about 16, for the same incident proton beam.

So, the secondary particle flux incident on Pt foil I_{sec}^{Pt} relative to primary proton beam is

$$\frac{I_{sec}^{Pt}}{I_p} = \frac{6.7 \cdot 10^6}{2.8 \cdot 10^{11}} = 2.4 \cdot 10^{-5} \quad (16)$$

practically it is the same as (13).

On the other hand, the inelastic π^+ and π^- nuclear interaction cross section for 1.5 GeV is smaller than proton – nucleus interaction for 24 GeV.

$$\pi^+ p(tot, 2\ Gev) = 30\ mb\ ;\ \pi^- p(tot, 2GeV) = 30\ mb \quad (17)$$

$$pp(tot, 24GeV) = 50\ mb \quad (18)$$

Acknowledgments

We want to thank to Juerg Schacher, Fujio Takeutchi and Soichiro Aogaki for useful discussions.

References

[1] L.Afanasyev „Pt foil integral measurements", DIRAC presentation (2011)

[2] A. Lanaro, „DIRAC Beam Parameters", DIRAC Note 2002-02.

[3] V.Brekhovskikh „Magnet & Pt foil Control System", DIRAC presentation (2012).

[4] O.E. Gortchakov et al., Yad. Fiz. 59 (1996) 2015.